2013 IEEE International Conference on Robotics and Automation (ICRA)
Karlsruhe, Germany, May 6-10, 2013

Adaptive mission planning for cooperative autonomous maritime vehicles

Gabriele Ferri and Vladimir Djapic

Abstract— **This paper addresses the problem of developing an autonomous cooperative multi-vehicle system composed of one simple low-cost unmanned underwater vehicle (UUV) guided by a more capable, sensor-equipped, surface or underwater vehicle. Specifically, in this work we consider a system composed of an autonomous surface vehicle (ASV) able to localize a small-sized UUV via a multibeam sonar and, then, to guide it via an acoustic link to reach a target. The UUV is equipped with low-cost navigation sensors (a compass and a depth sensor), and to estimate its own position relies on the data received by the ASV (range and bearing from the ASV and ASV position). This paradigm was applied in the domain of mine countermeasures (MCM) to realize the NATO CMRE Autonomous Mine Neutralization System. In this system the low-cost feature of the UUV is of the most importance since the UUV is supposed to be expendable. In this approach, however, there may be cases in which the underwater vehicle cannot be detected by the sonar for extended time periods causing drifts in the UUV position estimate, potentially compromising the mission. This paper presents a set of behaviors to address this situation. The behaviors coordinate ASV circular search patterns together with sending to the UUV purposely generated navigation updates. The aim is to limit the distance between the two vehicles, increasing the probability of sonar reacquisition, and at the same time ensuring that the UUV progresses toward the target. Results from sea trials held in Elba island (Italy) during ANT12 experiments (in June 2012) are reported, and demonstrate the approach is effective and can push our system toward full autonomy.**

I. INTRODUCTION

Nowadays, accurate autonomous underwater navigation is guaranteed for marine vehicles by the use of expensive sensor suites. Usually, an aided inertial navigation system (AINS) is installed onboard to produce the needed localization data. AINS systems integrate an inertial measurement unit (IMU) with a Doppler velocity log, a depth sensor and an underwater or global positioning system [1]. Aiding sensors are needed to limit the drift rate or periodically reset the errors in the position estimates during the navigation. Long baseline (LBL) systems can provide position fixes with a subcentimeter precision and update rates up to 10 Hz [2]. However, in these systems, LBL transponders need to be precisely moored to the seafloor to create the acoustic polygon. The use of moored GPS intelligent buoys (GIB) [3] can guarantee a sufficient localization performance without the need of precise mooring. Nevertheless, the placement and recovery of transponders remain necessary, and the area covered by the positioning system is fixed once the acoustic polygon is set.

To avoid these limitations and to reduce the need for navigation sensors onboard the UUV, a different approach based on the use of cooperative autonomous vehicles can be pursued. In this approach the UUV is guided via an acoustic link by a more capable, sensor-equipped vehicle providing the UUV with the information needed for an accurate navigation to a target. The more capable vehicle can be either an expensive AUV equipped with the needed sensor suite [1] or an ASV. ASVs with capabilities of long range missions and safe navigation in real environments are nowadays becoming available, and represent relatively low-cost and versatile solutions for a large set of applications [4]; in particular, as a communication relay for a companion underwater robot [5] and as support to the UUVs navigation.

Following this concept, a system for mine neutralization [6] was realized at CMRE composed of two cooperating autonomous vehicles: a small-sized, low-cost UUV, supported in its navigation by a "mother" ASV autonomously navigating to keep the distance to the underwater vehicle limited.

A method has to be selected to compute the localization information needed by the UUV. One possibility is to adopt an ultra short baseline (USBL) [2] system located on the support platform. The USBL performance, however, degrades with higher elevation angle, especially observed in shallow waters. To avoid this problem we opted for a multibeam sonar mounted on the ASV tracking the UUV. The higher multibeam resolution offers better precision in comparison to USBL measurements and does not require precise mooring of transponders as in LBL systems. The drawback in this approach is that the UUV has to remain inside the sonar field of view (FOV) to be tracked. For this reason, the sonar is mounted on a pan-and-tilt system.

Nevertheless, the UUV sometimes may be "lost" by the tracking ASV. This may happen either in the case of the UUV exiting the sonar FOV or in the case of some errors/failures in the automatic image processing. In these cases the UUV has to be reacquired commanding the tilt/pan of the sonar and/or the ASV position to avoid drifts and large localization errors during UUV navigation. An automatic strategy for reacquiring the UUV is needed to have a system completely autonomous.

This paper describes a set of behaviors for the ASV addressing this issue. In case the UUV has not been detected

This work was performed under the 2011-2012 NURC/CMRE CPOW, and supported by the Centre's Visiting Researcher Programme.

G. Ferri is with the NATO Centre for Maritime Research and Experimentation (CMRE), Viale San Bartolomeo 400, La Spezia, Italy ferri@cmre.nato.it

V. Djapic is with the NATO Centre for Maritime Research and Experimentation (CMRE), Viale San Bartolomeo 400, La Spezia, Italy djapic@cmre.nato.int

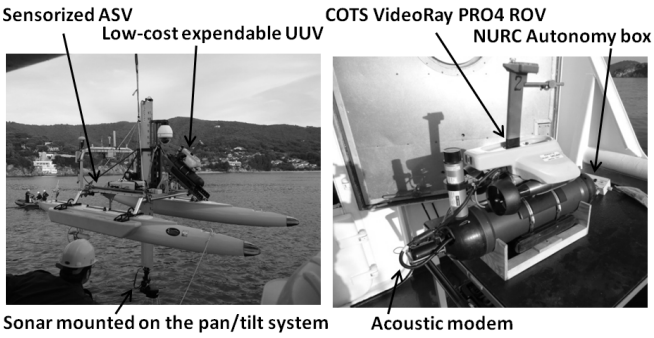

Fig. 1. The CMRE system of cooperative maritime vehicles. The system is composed of a "mother" autonomous ASV that deploys a low-cost "daughter" automatic UUV and guides it acoustically to a target.

for a certain time, the ASV initiates a circular search pattern and sends acoustic data to command "fake" positions to the UUV localization software to force its movement. The acoustic data are created based on the ASV location and aim at generating a zig-zagging movement of the UUV. These commands serve to limit the distance between the two vehicles and increase the likelihood of sonar reacquisitions while ensuring the UUV progresses toward the target even when the sonar tracking data are not available. These behaviors are essential for our system of cooperative maritime vehicles to be truly autonomous, especially if we aim to adapt the envisioned concept of operations by substituting the surface vehicle with an AUV equipped with accurate navigation sensors. In that case, human intervention is not possible at all, and the system must work robustly in a fully autonomous way.

II. CMRE System of Cooperative Maritime Vehicles

The CMRE system of cooperative maritime vehicles (Fig. 1) is based on the marsupial robotics paradigm, and is composed of two vehicles working in a master-slave scenario in which the master surface vehicle is guiding the slave to the target [6]. It is composed of:

- A "mother" ASV that deploys a small expendable UUV, which it tracks via sonar and guides acoustically to the target.
- The "daughter" is an expendable, small-sized, low-cost UUV deployed by the ASV (or some other means) which carries the mission payload to the target. This vehicle is not equipped with sensors to determine its location on its own.

The general idea is, therefore, to have one autonomous vehicle (in this case the ASV) guiding one automatic vehicle (the UUV) to accomplish this, typically short (2-5 min), mission. The automatic vehicle is provided with capabilities of navigation, but relies on the autonomous vehicle for its localization and for receiving mission commands [6].

A. The autonomous ASV

The autonomous ASV is a modified SeaRobotics USV-2600 4-meter catamaran with two independently controlled propellers for its propulsion. It is equipped with accurate onboard sensors for self-localization and navigation: a DGPS, attitude sensors, a compass and a yaw rate gyro. A forward looking 2D multibeam sonar BlueView P900-130 is mounted on a pan/tilt system and was installed on the ASV. The sonar presents a wide horizontal FOV (130°) and a vertical beam width of 15°. The useful maximum range of the sonar can be considered 35 m, since at this distance the image processing succeeded in localizing the UUV robustly in sea trials [7]. Furthermore, a Florida Atlantic University (FAU) DPAM acoustic modem or a Woods Hole Oceanographic Institution (WHOI) micro-modem were added for the communication with the UUV.

B. The automatic UUV

The automatic UUV is a modified version of the Video Ray Pro 4 ROV (see Fig. 1). This vehicle is equipped with 2 horizontal and 1 vertical thrusters; a compass and a depth-sensor for navigation. An additional hull was attached to the bottom of the vehicle to contain a PC board, batteries and an acoustic receiver. Details about the modified Video Ray Pro 4 ROV are reported in [7].

C. Cooperative autonomous vehicles mission

A mission of our system for mine countermeasures is composed of three phases:

1) an area survey using AUVs or ASVs equipped with high-resolution sonars or synthetic aperture sonars [8] is performed to localize and confirm a prospective target;
2) the autonomous ASV is commanded to reach a location close to the target ($\sim$ 50 m) to reacquire the target using its sonar and to start the neutralization mission. The ASV deploys the automatic UUV;
3) the UUV follows a 3D line joining its starting position to the target by using the received range/bearing from the ASV to estimate its own position.

The range/bearing of the UUV are automatically computed from the 2D images [7]. The data are sent together with the current ASV position to the UUV via the acoustic modem. When received, this information is used together with the onboard pressure sensor depth data to produce an estimate of the vehicle position [7]. The frequency of the received measurements varies due to the communication channel, but has a minimum value of 0.5 Hz. The position estimates are fed to an Extended Kalman Filter running onboard the UUV and estimating the robot state (output frequency 10 Hz) [7]. The data received from the ASV limit the drift of the position estimate. This approach has been demonstrated through extended sea trials [7] to be appropriate to guide the UUV in an accurate way along a 3D line to the target. Details about the UUV guidance algorithm are reported in [7].

Here we just give an idea of the general structure of the guidance algorithm since this will be used in the realization of the ASV reacquisition strategy. The UUV divides the 3D line-following problem into two separate 2D line-following problems [7] while moving at a fixed surge speed u as shown in Fig. 2: the horizontal line l_H with d_H minimized

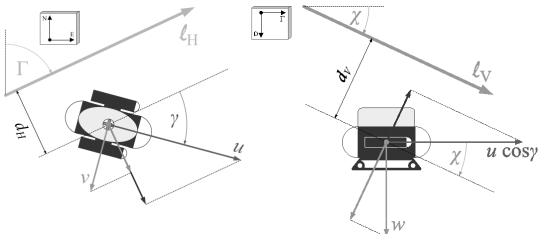

Fig. 2. The 3D line-following decomposition: (left) horizontal line following - d_H is minimized by controlling the heading angle ψ and (right) vertical line following - d_V is minimized by controlling the heave speed w.

by controlling the heading angle ψ, and the vertical line l_V with d_V minimized by controlling the heave speed w. During the mission the user (via a WiFi link) or the mission planner onboard can command the ASV two different movements: *keep-distance* (the ASV moves to keep a certain distance from the tracked UUV), or *circle-around* (the ASV performs a circle around an inspection point represented by the last estimated UUV position). The main features of our approach are the following:

- One-way communication from the ASV to the UUV is used.*
- The multibeam sonar of the ASV does not always need to keep the target and the UUV in the FOV, but only the UUV.
- If the ASV drifts due to water currents, the UUV movement will not be affected, and it will keep navigating along the line which has been determined initially.

III. Adaptive mission planning algorithm

The state diagram of the adaptive mission planning algorithm is shown in Fig. 3. During the mission, the ASV moves according to the movement commands received by the user or the mission planner (keep-distance, circle-around), tracks the UUV via the sonar and sends acoustically the localization data and commands to the UUV. The reacquisition algorithm intervenes in case the UUV has not been detectable (UUV "lost") by the sonar for a certain time. The ASV starts the mission setting the tilt angle for the sonar at 5 °and goes into the *tracking* state.

A. UUV TRACKING

This is the operational state while the UUV is detectable. If user commands are sent, they are accepted and the ASV consequently navigates. While moving, the sonar is actuated in tilt and pan by a tracking algorithm to keep the current UUV estimated position in the center of sonar FOV. Meanwhile, the sonar images are processed to detect the UUV [7]. In the case of detection, the measured range and bearing are sent to the UUV, and a new (x,y,z) position estimate of the UUV is computed onboard the ASV, becoming the new inspection point. The new position estimate is created by combining the measured range/bearing with the ASV position [7]. However, the sonar image is bi-dimensional so the ASV needs to know the depth of the UUV to estimate its position.

*Our aim is evaluate the possibility of using one-way simple acoustic receiver in future not the full capability acoustic modem as the modem is the only relatively expensive component on our current UUV configuration.

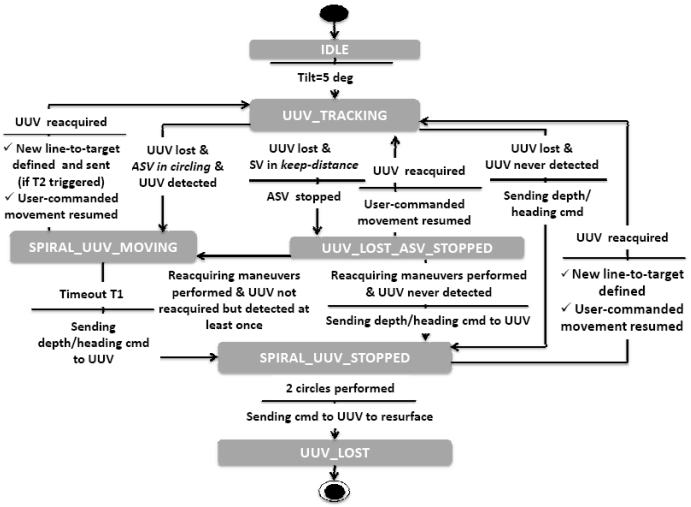

Fig. 3. State diagram of the adaptive mission planning algorithm.

The one-way link prohibits the UUV from sending its depth; the ASV therefore needs to make some assumptions. On the basis of the UUV operational states, commanded by the ASV via the acoustic channel, two depth estimate methods are used. If the UUV is commanded to reach a certain depth and a certain heading (*depth-heading* UUV state), the ASV assumes the UUV z-coordinate to be the commanded depth, since the UUV will dive to the received reference value. When the UUV is commanded to reach the target (*line-following* UUV state), the ASV estimates the depth on the basis of the current sonar tilt angle s_{θ_i} and by assuming the underwater vehicle is trying to follow the 3D line, minimizing its distance to the ideal trajectory to the target. That is,

$$min_{s_\theta \in [s_{\theta_i}-\theta_0, s_{\theta_i}+\theta_0]} \frac{||\boldsymbol{p}(\boldsymbol{p_{ASV}}, s_\theta, R, \varepsilon) \wedge \boldsymbol{l}||}{||\boldsymbol{l}||} \quad (1)$$

where s_θ is the sonar tilt angle that varies in an interval around the current tilt angle s_{θ_i} to minimize the angle between the line $\boldsymbol{p}(\boldsymbol{p_{ASV}}, s_\theta, R, \varepsilon)$ joining the start position of the 3D line and the estimate of the UUV position (depending on current ASV position $\boldsymbol{p_{ASV}}$, sonar range R, tilt angle s_θ and bearing ε) and the 3D line $\boldsymbol{l}$ to be followed.

At the beginning of the mission, the UUV is commanded to reach a certain depth and a certain heading with a *depth-heading* command. The UUV is detected by the ASV and starts receiving the localization data to correct its position estimate; then the ASV sends the UUV the coordinates of the target (*set-up target* command) and a message to follow a line. The UUV enters the *line-following* state: a 3D line is created from its current position to the target and it starts following the path. The *UUV tracking* state is exited in case the UUV is "lost", that is, the underwater vehicle has not been detectable by the sonar for more than ΔT seconds (a value of 7 s was considered, implying at least 3 consecutive sonar pings without detections).

B. UUV LOST ASV STOPPED

This state is entered when the UUV is "lost" and the ASV is moving according to the keep-distance primitive. First the

ASV starts a station-keeping maneuver and then evaluates the possible causes for the UUV loss. On the basis of the last measured range and bearing, different reacquisition actions are undertaken:

- High measured range (more than 2/3 of the maximum sonar range. In this case it is assumed the UUV has navigated outside of the sonar range, and the ASV moves toward the last inspection point for 10 m to reacquire the underwater vehicle.
- The last measured bearing is high ($> 50°$) or low ($< -50°$): in these cases the sonar pan angle is incremented (or decremented) with 2 steps of 25°.
- As default, the UUV is assumed to have exited the vertical sonar FOV since this is considered the most likely cause to lose the tracking. In this case, the ASV increases the sonar tilt angle with steps of 3°to reacquire the UUV (8,11,14°).

If the described reacquisition maneuvers succeed, the ASV comes back into the *UUV tracking* mode and resumes the movement received by the user. Otherwise, the ASV enters other states in which circular search patterns are run to detect the UUV (see Fig. 3).

C. SPIRAL UUV MOVING

This state is entered when the ASV is circling and the UUV is "lost", and represents the core state of the reacquisition strategy (see Fig. 3). The ASV starts a circular search pattern centered at the inspection point panning and tilting the sonar at this location. The ASV creates range/bearing data and sends them to the UUV to force movement toward the target, and confined inside two limiting lines lying on the $x-y$ plane and parallel to the horizontal projection of the predetermined 3D line to the target. Thus the UUV movement is combined with the ASV maneuvering to limit the distance between the two vehicles. This guarantees:

1) an increase of the probability of reacquiring the UUV (limiting distance), and
2) at the same time continuing the mission (the UUV is heading toward the target).

To achieve these objectives the range/bearing data are created based on the current ASV position along the circular trajectory. They are computed by considering "fake" (x,y) positions of the UUV, the ASV (x,y) coordinates and the estimate of UUV depth. The created range/bearing imply the UUV updates its (x,y) position estimate with the desired "fake" locations. The UUV induced "fake" positions span along the r line segment (see Fig. 4): r lies in the $x-y$ plane, passes through the inspection point and is perpendicular to the horizontal projection t of the desired 3D path to the target that intersects it at the middle point P. Since the UUV guidance algorithm minimizes (see Fig. 2) the lateral distance d_H to the horizontal line l_H (in this case t), by changing the "fake" positions along the r line, we can command the UUV to move in a desired way. The adopted strategy is shown in Fig. 4. With the ASV moving on one semicircle, the "fake" position is located in the other semicircle (Fig. 4a and Fig. 4c). In particular, an induced position estimate as in Fig. 4a generates a counter-clockwise turning of the UUV toward t to minimize the horizontal distance to t. If the ASV is moving on the arcs of the circle identified by the angle θ_0, the position is fixed at the point P (Fig. 4b), implying for the UUV a movement parallel to t. Since the UUV surge speed is kept constant and > 0, by purposely changing the "fake" position along r, a zig-zag movement of the UUV can be achieved. The zig-zag presents an overall resulting motion following the line d lying on the $x-y$ plane, parallel to t and passing by the last estimated UUV position (see Fig. 4). The horizontal distance from d is in this way kept bounded.

To avoid abrupt turning in the UUV navigation, the "fake" positions are changed smoothly along the r segment. They are changed proportionally to the angle α (shown in Fig. 4a): the maximum distance along the r segment is set with $\alpha = \pm 90\ °$, then the "fake" position slides on r toward the point P as the ASV progresses on the circle, and is set at P when the ASV is on the arcs of the circle identified by θ_0. During the zig-zag movement, the UUV does not change depth since its localization algorithm assumes not having moved forward along the 3D line (on the basis of the received data the estimated positions are along the r line perpendicular to t). The UUV, in fact, computes as its reference depth the z-coordinate of the 3D line to the target corresponding to the (x,y) coordinates of the P point.

To take into account the UUV movement toward the target, the center of the circle is moved as time passes (after T_3 s) along d (toward the target position) becoming the new inspection point I_1. The new sent data (coherent with "fake" positions along r_1) imply also a depth change of the UUV: the UUV dives at the z-coordinate of the 3D line to the target corresponding to the (x,y) coordinate of P_1. All this information is used to update the inspection point in the z-coordinate (used by the automatic tilting). The described method implies the following features:

- The zig-zagging UUV movement heads toward the ASV position along the circle keeping the distance between the two vehicles limited to increase the probability of a reacquisition. This also opposes to possible drifts caused by the water current pushing away the UUV from the ASV. Furthermore, the ASV, by changing the inspection point, follows the movement of the UUV toward the target.
- The overall UUV movement follows d and is limited inside the limiting lines: the UUV navigation is not interrupted and the mission continues.
- The circle search pattern gives the sonar the possibility to observe the UUV under different angles of view making the detection easier; this kind of search pattern can be also used if a nonholomic and underactuated torpedo-shape AUV is used in the place of the ASV since this kind of AUV has to keep moving to keep controlling its depth and track the UUV.
- The UUV depth is indirectly controlled: when a new inspection point is considered and a new r_1 is used to create localization data, a new depth reference is

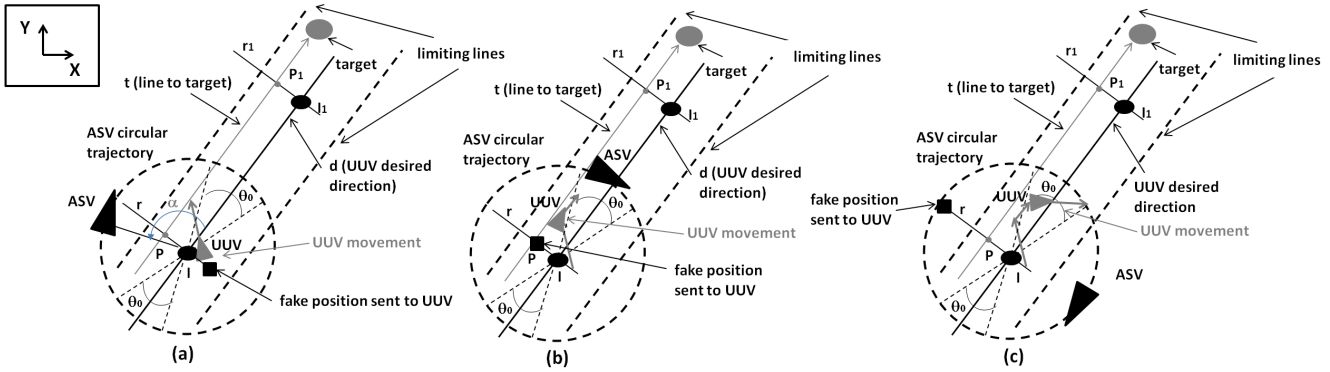

Fig. 4. Coordinated ASV and UUV movements diagram. The images shows the movements of the UUV on the base of the created "fake" positions. Sending range/bearing data coherent with different "fake" positions forces a zig-zag movement of the UUV; the overall movement follows the line d and is confined inside the two limiting lines.

implicitly sent to the UUV approaching this way the target depth.

The state is exited if the UUV has not been detected and a timeout T_2 triggers (into the *spiral uuv stopped* state) or in the case of a reacquisition (into the *tracking* state). In the case of reacquisition, the ASV sends a set-up target message and the UUV creates a new 3D line (if a certain time T_1 has passed since the start of the search pattern) from the new estimate UUV position to the target. This aims at directing the UUV toward the target in the cases it drifted far from the desired originally determined path.

D. SPIRAL UUV STOPPED

In this state the ASV sends the UUV a depth/heading command. The depth is set to a predefined value based on the target depth, and the commanded heading angle is that of a line joining the ASV position at the entrance of this state and the target. With these commands the UUV sets the surge speed to zero, moves at the received depth and rotates at the reference heading angle. The ASV updates the inspection point z-coordinate assuming the predefined commanded UUV depth, and performs two consecutive circles with increasing radii to explore the area. This represents the last attempt to localize the UUV. In case of the UUV is not detected, the UUV is considered definitely lost and a command of resurfacing is sent. If the UUV is detected a new set-up target is commanded and the ASV enters again the *tracking* state, resuming the user-commanded movement.

IV. SYSTEM SOFTWARE ARCHITECTURE

The software architecture of the CMRE system of cooperative vehicles is based on MOOS-IvP [9]. MOOS-IvP is an open source C++ framework for providing autonomy to robotic platforms, in particular marine vehicles. MOOS-IvP is based on the mailbox paradigm: a community of processes subscribe to receive and publish variables from/to a database (MOOSDB). For the control of vehicles, the MOOS framework works according to the backseat-driver paradigm: a backseat computer executes the processes managing the mission and produces commands for a frontseat computer in charge of the vehicle low-level control [9].

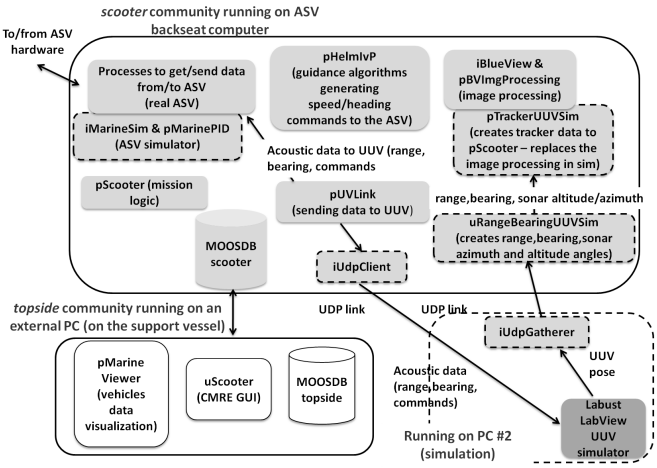

Fig. 5. Scheme of the system software architecture based on MOOS-IvP middleware(the different processes are shown). The *pScooter* process manages the mission logic and commands navigation behaviors to *pHelmIvP*. The simulation environment is shown with the related processes characterized by dashed contour. The UUV simulator, developed in Labview (the onboard UUV control sofware is used), is run on PC #2. The two computers communicate via an Ethernet channel by using UDP sockets.

In our system, the MOOS community managing the ASV mission produces commands (heading and surge speed references, acoustic commands to the modem, etc.) for the different ASV hardware components such as the acoustic modem and the vessel frontseat computer. In Fig. 5 a scheme of the main processes of our system is shown. The community on the ASV (*scooter*) communicates also with the *topside* community that provides a graphical interface to the user to visualize the robots' movements and to send commands to the ASV. To test the software to be used onboard the vehicle we developed several processes to simulate missions involving both vehicles' operations. *uRangeBearingUUVSim* and *pTrackerUUVSim* processes, for instance, replace in simulation the processing of real sonar data by producing sonar detections of the UUV. To simulate the UUV, a software running on PC#2 was used to generate the UUV position data. The software was realized in LabVIEW (NI^{TM}) by the LABUST from Univ. of Zagreb, and is composed of the onboard UUV control software and of a dynamic model of the vehicle [7]. It receives the acoustic data produced by the ASV and behaves accordingly. The MOOS-IvP helped

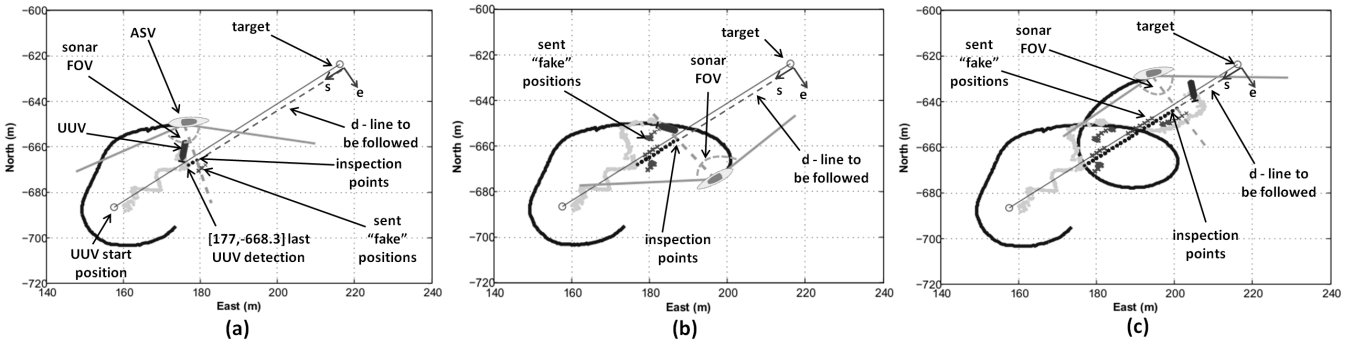

Fig. 6. Results of a sea trial. The $x-y$ positions of the two vehicles are shown at different mission times together with the "fake" positions and the inspection points moving along d to follow the UUV movement. The sonar FOV is shown with the dashed grey line representing the effective sonar range (35 m). The reacquisition movement starts when the UUV is located at (177,-668.3). This is visible in (a) in which the UUV is heading toward the ASV decreasing the ASV-UUV distance. The UUV moves toward the target with an overall motion following the line d.

the process of developing and integrating new software, and allowed us to easily test and tune the onboard code.

V. Experimental results

Simulation sessions were carried out to investigate the performance of the proposed behaviors as the parameters change. To simulate a realistic interaction between the vehicles, we considered the latency and the delays in communication appropriate to the acoustic channel (the acoustic communication frequency is 0.5 Hz), and a first order model was included to simulate the dynamics of the motors controlling the sonar tilt/pan with a maximum rotation speed of 20 °/s. Numerous simulations showed the feasibility of the approach and provided insight on how to set the algorithm parameters. Thanks to the MOOS structure, the software, after being validated in simulation, was easily ported on real vehicles to be tested at sea and we will present those results.

We validated the algorithm in costal area of Elba island (water depth up to 15 m, negligible water currents), Italy, during the ANT12 (Autonomous Neutralization Trial 2012). ANT12 experiments were conducted with the major objective to test and validate the complete autonomy of operations of the CMRE Autonomous Mine Neutralization System. As a secondary objective we carried out some missions to test the method presented in this work. We discuss the results of one of these trials in which a sonar loss was simulated. In this trial, the target was a truncated cone type mine positioned on the seafloor at a depth of 5 m. In Fig. 6 the two vehicles' positions are plotted at different times of the trial. ASV positions were provided by onboard DGPS, while the UUV positions were computed off-line by using stored ASV positions and sonar data. The UUV was deployed by the ASV 86 m south-west of the target (see Fig. 6a). Then, the ASV commanded the line-following behavior to the UUV, which then started moving toward the mine (see Fig. 6a). During the line-following the ASV navigated in circle-around mode around the UUV. In this phase the UUV was automatically tracked by sonar and sonar data were acoustically sent to the UUV for its navigation.

When the UUV was at position (177,-668.3) (see Fig. 6a) we simulated a sonar loss: sonar data were not used from this point on by the ASV, but were logged to compute the UUV ground-truth position off-line after the trial conclusion (in the reacquisition phase we assumed as UUV depth the z-coordinate of the 3D line to the target corresponding to the sent "fake" positions – see Sec. III-C) . The ASV entered the *spiral UUV moving* state and circled around the inspection point sending "fake" positions to the UUV. The radius of the circle was set to 12 m, considering the effective sonar range (35 m), and was a trade-off between area exploration (larger radius) and area coverage (smaller radius). The inspection point was moved along line d 1.5 m every 5 s. The "fake" positions and the inspection points progressing along d are visible in the figure. Finally, automatic pan/tilt was active and the sonar was pointed automatically to the current inspection point. The UUV zig-zags around d heading toward the current ASV position along the circle with its motion remaining laterally limited (see Fig. 6).

The UUV was driven in this way for a time of 2 minutes along the line d toward the target for more than 40 m, diving to the target depth. During the descent, the UUV depth followed the z-coordinate of the 3D line to the target, indirectly commanded by the received data (this is visible from the data logged by UUV). The UUV along-track speed (along d and toward the target position) was on average 0.34 m/s guaranteeing a sufficiently fast navigation to the mine. During the path, the UUV always remained inside the sonar FOV and within the sonar range (in Fig. 6 the sonar FOV is shown together with the effective range – dashed central line of the sonar beam). Numerical results of the trial are reported in Tab. I. The ASV-UUV 3D distance (shown in Fig. 7) presents a maximum value of 31.4 m with an average of 23.4 m during the entire path, guaranteeing the possibility of UUV detection by image processing. The zig-zag movement causes periods of particularly reduced distance (e.g. around time 855 s and 960 s - see Fig. 6a and Fig. 6c) increasing the sonar reacquisition probability. The selected parameter set resulted in satisfying results also by looking at the cross-track error (e), reported in Fig. 8, defined as the lateral error with respect to d (see the $s-e$ reference frame in Fig. 6). The maximum value of e during the whole reacquisition phase is -14.3 m with an average value of -3.2 m. The lateral movement is bounded and the negative average value is due to the positions of the UUV and ASV at the start of *spiral UUV moving* state.

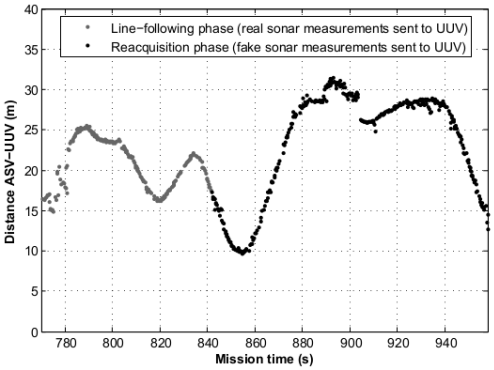

Fig. 7. 3D distance between the ASV and the UUV during the line following (in gray) and the reacquisition phase (in black).

In general, 3D distance and e evolution depends on different parameters and can be modified by varying the circle radius, vehicles speed, or the inspection point change policy. In particular, the key parameter to be set is the speed of the inspection point movement along the path. Ideally, this point has to be changed on the basis of the UUV along-track speed to have the centers of the covered circles following the projection of the UUV position on the line d, in order to keep the UUV in the middle of sonar FOV. If the inspection point is not updated accordingly, the distance between the vehicles increases and the UUV may exit from the sonar FOV. In our trial we can observe the ASV followed the UUV path well for a distance of 40 m (47 % of the length of the path to be covered in the mission) guaranteeing a time of 2 minutes to the image processing to produce again a reliable track of the underwater vehicle.

However, we can note that at the end of the experiment (Fig. 6c) the UUV is about 6 m ahead of the last inspection point showing a slight difference between the inspection point update speed and the UUV along-track speed (~ 0.05 m/s). The UUV along-track speed can be correctly computed by knowing all the algorithm parameters and having an accurate estimate of UUV surge speed. Nevertheless it can be influenced by the presence of water currents. For this reason, we are investigating how to take into account the current speed in the update of the inspection point to give more time to the image processing to track the UUV again by keeping the UUV close to the center of sonar FOV.

VI. Conclusion

Sea trials demonstrated the practical viability and effectiveness of the proposed approach. The acoustic data combined with the ASV circling force the UUV to navigate zig-zagging with an overall motion following a line parallel to the $x-y$ projection of the desired 3D path to the target. The movement is characterized by a bounded cross-track error and the UUV heads toward the current ASV position to limit the distance between the vehicles increasing sonar detection probabilities. In the case of UUV losses by the image processing, the mission can continue until a sonar reacquisition occurs. The UUV was guided without the use of sonar data for a path of 40 m with a mean along-track speed of 0.34 m/s. The UUV was always in the sonar FOV

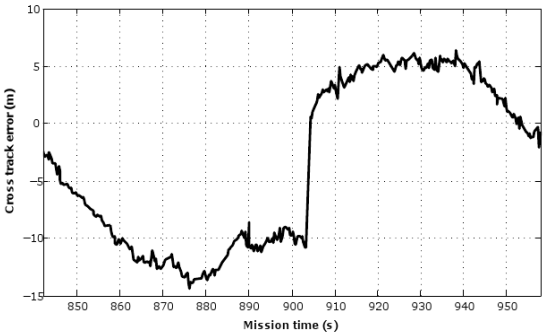

Fig. 8. Cross track error (e) during the reacquisition phase.

TABLE I

Reacquiring phase time [m]	Distance ASV-UUV [m]	Cross-track error (e) [m]	Effective UUV speed (|ds/st|)
2	μ=23.4, σ=6.5 max range = 31.4	μ= -3.2, σ=6.8 max(|e|)=14.35	μ= 0.34 m/s

and within the sonar range giving the image processing algorithms a time of 2 minutes for the reacquisition.

The seas were mild and in future we plan on testing in rougher conditions. To increase the length of the path, a key factor is to take into account sea currents speed. Sea currents, in fact, can both induce a drift in the UUV lateral motion (e) and can modify the UUV along-track speed implying a different needed policy for the update of the inspection point along the path. For these reasons, an ADCP sonar is under integration in the ASV and will be available to produce an estimate of the water currents speed to be used in the algorithm to limit the UUV lateral drift and to change the inspection point more coherently with the real UUV position.

Acknowledgment

The authors want to thank Alberto Grati and Stefano Fioravanti for their invaluable engineering support and the CMRE ETD staff for their helpfulness during ANT12 trials.

References

[1] P.A. Miller, J.A. Farrell, Yuanyuan Zhao and V. Djapic, Autonomous underwater vehicle navigation, *IEEE Journal of Oceanic Engineering*, vol. 35(3), 2010, pp 663–678.

[2] J. C. Kinsey, R. M. Eustice and L. L. Whitcomb, A survey of underwater vehicle navigation: recent advances and new challenges, *Proc. of MCMC 2006*, Lisbon, 2006.

[3] A. Alcocer, P. Oliveira and A. Pascoal, Study and implementation of an EKF GIB-based underwater positioning system, *in IFAC CAMS04*, 2004.

[4] G. Ferri, A. Manzi, F. Fornai, B. Mazzolai, C. Laschi, F. Ciuchi and P. Dario, Design, fabrication and first sea trials of a small-sized autonomous catamaran for heavy metals monitoring in coastal waters, *in Proc. of ICRA 2011*, Shanghai, China, May 2011.

[5] A. Pascoal et al., Robotic ocean vehicles for marine science applications: the European ASIMOV project, *in Proc. of Oceans 2000*, Providence, RI, USA, 2000.

[6] V. Djapic and D. Nad, Collaborative Autonomous Vehicle Use in Mine Countermeasures, *in Sea Technology Magazine*, Nov. 2010, (http://www.sea-technology.com/features/2010/1110/autonomous_vehicle.php).

[7] D. Nad, N. Miskovic, V. Djapic and Z. Vukic, Sonar Aided Navigation and Control of Small UUVs, *in 19th Mediterranean Conference on Control and Automation (MED)*, Corfu (Greece), 2011, pp. 418-423.

[8] L. A. Mayer, R. Raymond, G. Glang, M. D. Richardson, P. Traykovski and A. C. Trembanis, High-Res resolution Mapping of Mines and Ripples at the Martha's Vineyard Coastal Observatory, *in IEEE Journal of Oceanic Engineering*, vol. 32, no. I, January 2007, pp 133-149.

[9] http://oceanai.mit.edu/moos-ivp/pmwiki/pmwiki.php.